

# Dark energy stars: Stable configurations

Piyali Bhar\*

*Department of Mathematics, Government General Degree College, Singur, Hooghly 712 409, West Bengal, India*

Tuhina Manna†

*Department of Commerce (Evening), St. Xaviers College,  
30 Mother Teresa Sarani, Kolkata 700016, West Bengal, India*

Farook Rahaman‡ and Ayan Banerjee§

*Department of Mathematics, Jadavpur University, Kolkata-700032, India*

(Dated: May 12, 2022)

In present paper a spherically symmetric stellar configuration has been analyzed by assuming the matter distribution of the stellar configuration is anisotropic in nature and compared with the realistic objects, namely, the low mass X-ray binaries (LMXBs) and X-ray pulsars. The analytic solution has been obtained by utilizing the dark energy equation of state for the interior solution corresponding to the Schwarzschild exterior vacuum solution at the junction interface. Several physical properties like energy conditions, stability, mass-radius ratio, and surface redshift are described through mathematical calculations as well as graphical plots. It is found that obtained mass-radius ratio of the compact stars candidates like 4U 1820-30, PSR J 1614-2230, Vela X-1 and Cen X-3 are very much consistent with the observed data by Gangopadhyay et al. (Mon. Not. R. Astron. Soc. 431, 3216 (2013)). So our proposed model would be useful in the investigation of the possible clustering of dark energy.

PACS numbers:

## I. INTRODUCTION

In 2005 physicist George Chaplin proposed that, gravitational collapse of objects with masses greater than a few solar masses should lead to the formation of a compact object called *dark energy star* whose surface corresponds to a quantum critical surface for space-time, and whose interior differs from ordinary space-time only in having a much larger vacuum energy [1]. He claimed that the current picture of gravitational collapse as explained in terms of event horizon is physically inconsistent since it conflicts with quantum mechanics [2]. The theory states that infalling matter gets converted to dark energy as it falls through the event horizon causing the space inside the event horizon to have a high value of cosmological constant and hence a high negative pressure to exert against gravity. This high negative pressure may counter the mass the star gains thus avoiding a singularity. Thus there is a sort of phase transition occurring in the phase of space at the event horizon [2, 3]. In fact Dark energy star may account for high energy cosmic ray sources and positron sources since infalling masses decays into lighter masses at the event horizon accelerating proton decay. This proposal may provide a new perspective on spectacular astrophysical phenomena including supernovae explosions, gamma ray bursts, positron emission,

and dark matter.

There is hardly any other topic in general relativity which is as extensively researched as black holes. Since Oppenheimer and Snyder [4] first attempt at explaining the state of gravitational collapse of a black hole, there have been various observational data favouring the existence of event horizon, but nonsoever proving it [5]. This in turn has lead to the developement of a plura of fascinating alternative ideas. One such popular model is that of a gravastar or gravitationally vacuum star as proposed by Mazur and Mottola [6]. Its a compact object having an interior de Sitter condensate defined by the equation of state  $p = -\rho$ , matched to a shell of finite thickness with an equation of state  $p = \rho$ , which is again matched to an exterior Schwarzschild vacuum solution. This star has no singularity at the origin and no event horizon since the thick shell surface with a radius slightly greater than the Schwarzschild radius, replaces both the de Sitter and the Schwarzschild horizons. The charged and uncharged model of gravastar was obtained in our earlier works [7]. A modified version of the gravastar was studied by Cattoen *et al.* [8] using a continuous pressure profile without thin shells. It strongly suggested an anisotropic pressure model. Later an alternative model termed as Born-Infeld phantom gravastar was constructed replacing the de-Sitter spacetime by an interior spacetime governed by the Chaplygin gas equation of state [9]. In this paper the authors have investigated a generalized case in which the equation of state is governed by the equation of state  $p = \omega\rho$  matched to an exterior vacuum solution. The proposed stellar model consists of five zones : an interior core, a thin shell between the core and the interior

\*Electronic address: piyalibhar90@gmail.com

†Electronic address: tuhinamanna03@gmail.com

‡Electronic address: rahaman@associates.iucaa.in

§Electronic address: ayan7575@yahoo.co.in

spacetime, the interior spacetime and a thin shell which acts as a junction interface between the interior and the exterior Schwarzschild spacetime. This kind of compact object which generalizes a gravastar model by using equation of state  $p = \omega\rho$  with  $\omega < -1/3$  is called a dark energy gravastar or simply a dark energy star, as referred by Chapline. This terminology is motivated by the fact that dark energy is still unknown component of our Universe has relativistic negative pressure. The 1998 observations of Type Ia Supernova [10] confirms that dark energy is responsible for the phase of cosmic acceleration. Numerous other recent observations of Cosmic Microwave Background (CMB) anisotropies and Large Scale Structure (LSS) [11] reconfirm this characteristics of small redshift evolution of our Universe. The simplest explanation of dark energy is the cosmological constant  $\Lambda$  which is usually interpreted physically as a vacuum energy, with  $p = -\rho$ . Another possible way to explain the dark energy is by invoking an equation of state,  $p = \omega\rho$  with  $\omega < 0$ , where  $p$  is the spatially homogeneous pressure and  $\rho$  the energy density of the dark energy, instead of the constant vacuum energy density. The models of dark energy with  $\omega > -1$  mainly comprises of quintessence, k-essence and Chaplygin gas among others.

This idea of dark energy star theorizes that the surface of a compact object is a quantum critical shell with some thickness  $z$  [12]. When ordinary elementary particles which have energy beyond  $Q_0 = 100\text{MeV}\sqrt{\frac{M_0}{M}}$ , where  $M_0$  is the solar mass, enter this quantum critical region they decay into substituent products and radiation that gets directed backwards from the surface of dark energy star perpendicular to the critical surface. However for particles with energy  $< Q_0$  will pass through the critical surface and follow diverging geodesics in the interior of a dark energy star. Now compact objects at the centre of galaxies contains quarks and gluons inside nucleons whose energies exceed this value [13]. According to Georgi-Glashow grand unified model nucleons can decay by a process in which a quark decays into a positron and two antiquarks. Interestingly an excess of positrons have been detected in the centre of galaxies which may be the best evidence for dark energy stars. In addition to that, primordial dark energy stars can form out of fluctuations of spacetime analogous to a quantum critical instability [2]. This in turn can help us understand dark matter. Thus motivated dark energy star have been investigated in many notable work. In a pioneering paper Lobo [14] has given a model of a stable dark energy star by assuming two spatial types of mass function: one is of constant energy density and the other mass function is a Tolman & Whitaker mass. All the features of the dark energy star have been discussed and the system is found to be stable under a small linear perturbation. In our previous work a new model of dark energy star consisting of five zones, namely, the solid core of constant energy density, the thin shell between core and interior, an inhomogeneous interior region with anisotropic pressures, a thin shell, and

the exterior vacuum region is obtained [15]. Yadav *et al.* [16] have given a dark energy model with a variable equation of state parameter. Inspired by the prior mentioned works of Cattoen *et al.* [8] and Ruderman (1972) [20] we have taken the pressure inside the fluid sphere in our model to be anisotropic. For an anisotropy distribution, the pressure inside the fluid sphere is decomposed into two orthogonal components: radial pressure  $p_r$  and transverse pressure  $p_t$  where obviously  $p_r \neq p_t$ . Studies on X-ray pulsars, Her-x-1, X-ray buster 4U 1820-30, millisecond pulsar SAX J1804.4-3658 etc. suggests that nuclear matter tends to become anisotropic in nature at very high densities ( $10^{15}\text{gm/cc.}$ ) [21, 22]. Anisotropy may occur due to any of the following reasons: existence of solid core, a type 3A superfluid [23], phase transition [24], pion condensation [25], rotation, magnetic field, mixture of two fluid, existence of external field etc.

We organised the paper as follows: In Sec. II. deals with the basic field equations and their solutions, then the junction conditions have been discussed in Sec. III. In Sec. IV. the physical properties with the stability conditions have been studied. Finally, in Sec. V. we discuss some specific comments regarding the results obtained in the study.

## II. INTERIOR SPACE-TIME

We consider a static spherically symmetric space-time given by the following line element:

$$ds^2 = -\exp\left[-2\int_r^\infty g(\tilde{r})d\tilde{r}\right]dt^2 + \frac{dr^2}{1-\frac{2m}{r}} + r^2d\Omega^2, \quad (1)$$

where  $g(r)$  and  $m(r)$  are two arbitrary functions of the radial coordinate  $r$ . The function  $g(r)$  represent the locally measured gravitational acceleration, which is positive for an inward gravitational attraction, and negative for an outward gravitational repulsion and  $m(r)$  is the gravitational mass contained within a sphere of radius  $r$ .

We proceed now to describe the matter distribution of the spherical body which is anisotropic in nature, and the energy-momentum tensor is characterized by the following relationships

$$T_{\mu\nu} = (\rho + p_t)U_\mu U_\nu + p_t g_{\mu\nu} + (p_r - p_t)\chi_\mu \chi_\nu, \quad (2)$$

where  $U_\mu$  is the four-velocity and  $\chi_\mu$  is the unit spacelike vector in the radial direction. This interpretation can be justified by invoking the static stress-energy tensor  $T_\nu^\mu = \text{diag}[\rho, p_r, p_t, p_t]$ . Now, using the energy-momentum tensor for the metric given in Eq. (1), the Einstein field equation provides the following relationships (in relativistic units with  $G = c = 1$ )

$$m' = 4\pi r^2 \rho, \quad (3)$$

$$g = \frac{m + 4\pi r^3 p_r}{r(r - 2m)}, \quad (4)$$

$$p'_r = -\frac{(\rho + p_r)(m + 4\pi r^3 p_r)}{r(r - 2m)} + \frac{2}{r}(p_t - p_r), \quad (5)$$

where  $\rho(r)$  is the energy density,  $p_r(r)$  and  $p_t(r)$  are the radial and tangential pressures respectively and 'prime' denotes the derivative with respect to the radial coordinate,  $r$ . Equation (5), corresponds to the Bianchi identity implies that  $\Delta_\mu T^{\mu\nu} = 0$ , may also be obtained by using relativistic Tolman-Oppenheimer-Volkov (TOV) equation for anisotropic pressure.

Thus we have three equations, namely, the field equations (3)-(5), with five unknown functions of  $r$ , i.e.,  $\rho(r)$ ,  $p_r(r)$ ,  $p_t(r)$ ,  $g(r)$  and  $m(r)$ . Therefore, it is extremely difficult to obtain an explicit solution of Einstein field equations. But as in aforesaid discussion, we are interested in more realistic situation where the mass function is uniform and field distributions are simply obtained for determining the physical features of a compact star. With this aim in mind, let us assume that the mass density which increases from the star center ( $r = 0$ ) to the surface ( $r = R$ ) and an equation of state  $p = p(\rho)$ .

It is convenient at this point to introduce the mass and fluid with the equation of state in the particular form

$$m(r) = \frac{ar^3}{2} \left( \frac{2 + ar^2}{(1 + ar^2)^2} \right), \quad (6)$$

$$p_r = \omega\rho. \quad (7)$$

For the choice of mass function gives a monotonic decreasing matter density as used earlier by Singh et al.[31], for modelling a compact star of embedding class I. It will be suitable to express the physical variables in terms of metric function, and our anisotropic fluid configuration to be physically acceptable. Now, taking into account the Eqs. (3) and (4) and using the dark energy equation of state, we obtain

$$g(r) = \frac{ar}{2(1 + ar^2)} [2(1 + 3\omega) + (1 + \omega)(3ar^2 + a^2r^4)], \quad (8)$$

To study the nature of dark energy for local astrophysical manifestation has attracted a lot of interest and for excellent reviews on this topic see Ref. [17]. The existence of dark energy star makes us expect that it is a generalization of the gravastar picture with an interior solution governed by the dark energy EOS and such objects have received considerable attention in astrophysics though some steps in this direction have already been emerged.

Solving the above differential Eqs. (3-5), using dark energy equation of state  $p_r = \omega\rho$ , we obtain the physical

parameters for this model are then given by :

$$\rho = \frac{a}{8\pi} \left[ \frac{6 + a^2r^4 + 3ar^2}{(1 + ar^2)^3} \right], \quad (9)$$

$$p_r = \frac{\omega a}{8\pi} \left[ \frac{6 + a^2r^4 + 3ar^2}{(1 + ar^2)^3} \right], \quad (10)$$

$$p_t = \frac{a}{32\pi(1 + ar^2)^4} [24\omega + 12ar^2(1 + 2\omega + 3\omega^2) + 12a^2r^4(2 + 5\omega + 3\omega^2) + a^3r^6(17 + 38\omega + 21\omega^2) + a^4r^8(1 + \omega)^2(6 + ar^2)], \quad (11)$$

and the anisotropic factor  $\Delta$  is given by

$$\Delta = p_t - p_r = \frac{a}{32\pi(1 + ar^2)^4} [12ar^2(1 - \omega + 3\omega^2) + 4a^2r^4(6 + 11\omega + 9\omega^2) + a^3r^6(17 + 34\omega + 21\omega^2) + a^4r^8(1 + \omega)^2(6 + ar^2)]. \quad (12)$$

The anisotropy factor measures the pressure anisotropy of the fluid comprising the dark energy star. An isotropic pressure dark energy star corresponds to  $\Delta = 0$ . Here  $\Delta/r$  represents a force arising due to the anisotropic nature of the stellar model. The anisotropy will be repulsive or directed outwards if  $p_t > p_r$ , and attractive or directed inward when  $p_t < p_r$ . From the above set of solutions we observe that the central density,  $\rho_0 = 6a/8\pi$ , being a non-zero constant quantity, satisfies the regularity conditions and finite character at the origin.

We shall now analyze the energy density is positive and finite at all points in the interior of the star and some physical criterion which are necessary for the interior solution. Therefore, it is necessary to impose the restrictions on the constants appearing in the metric functions, so that all criteria for physical acceptability are satisfied and well behaved at all the inner points of strange stars. So, taking derivatives of Eqs. (9), (10) and (12) with respect to the radial coordinate, we have

$$\frac{d\rho}{dr} = \frac{a}{8\pi} \left[ \frac{6 - 30ar + 6ar^2 - 8a^2r^3 - 2a^3r^5}{(1 + ar^2)^4} \right], \quad (13)$$

$$\frac{dp_r}{dr} = -\frac{\omega a^2 r}{4\pi(1 + ar^2)^4} [15 + 4ar^2 + a^2r^4], \quad (14)$$

$$\frac{d\Delta}{dr} = \frac{a}{32\pi(1 + ar^2)^5} [24ar(1 - \omega + 3\omega^2) + a^2r^3(24 + 248\omega - 72\omega^2) + a^3r^5(6 + 28\omega - 18\omega^2) + a^4r^7(14 + 28\omega + 6\omega^2) + 2a^5r^9(1 + \omega)^2(5 + ar^2)].$$

Here, we observe that  $\frac{d\rho}{dr} = 0$  and  $\frac{dp_r}{dr} = 0$  at the origin, which clearly indicate that at the centre of the star, density is maximum and it decreases radially outward. We have also verified that the radial pressure is maximum at the centre and it decreases towards the boundary. Thus, the energy density is continuous and well behaved in the stellar interior has been shown in Fig. 1. One readily verifies from Figs. 2 and 3, that  $g(r) > 0$ , within the range of  $-1/3 < \omega < 0$ , indicating an inward gravitational attraction, and within the range of  $-1/3 < \omega < -1$ ,  $g(r)$

$< 0$ , shows an outward gravitational repulsion. Since, we are dealing with dark star, thus it is necessary that the interior solution must be repulsive in nature, so that the region where  $g(r) > 0$  associate with inward gravitational attraction is necessarily excluded.

The entire analysis has been performed with a set of astrophysical objects in connection to direct comparison of some strange/compact star candidates like X-ray pulsar Cen-X3, X-ray burster 4U 1538-52, and X-ray sources 4U 1538-52. In connection with that we extensively studied the physical features of compact star Vela X - 1.

### III. JUNCTION CONDITION

Now, we are instead in writing the junction conditions, where the space-time is matched to an exterior schwarzschild vacuum solution with  $p = \rho = 0$  at the junction interface  $\Sigma$ , with junction radius  $R$  is given by:

$$ds^2 = - \left(1 - \frac{2M}{r}\right) dt^2 + \frac{dr^2}{1 - \frac{2M}{r}} + r^2(d\theta^2 + \sin^2\theta d\phi^2), \quad (16)$$

which possesses an event horizon at  $r_h = 2M$ . We have choose the value of junction radius  $R > r_h$  to avoid the presence of horizons i.e., the junction radius lies outside  $2M$ . Here, we show that  $M$ , may be interpreted as the total mass of the dark energy star. Now using the standard Darmois-Israel formalism [18], the intrinsic stress-energy tensor  $S_{ij}$ , at the junction surface  $\Sigma$  is defined through the Lanczos equation as

$$S_j^i = -\frac{1}{8\pi} (\kappa_j^i - \delta_j^i \kappa_m^m), \quad (17)$$

where the quantity  $k_{ij}$  represents the discontinuity in the extrinsic curvature  $K_{ij}$  and the discontinuity is given by  $k_{ij} = K_{ij}^+ - K_{ij}^-$ . Each of the extrinsic curvatures and using the second fundamental form the extrinsic curvature can always be written as

$$K_{ij}^\pm = -\eta_\nu \left( \frac{\partial^2 x^\nu}{\partial \xi^i \partial \xi^j} + \Gamma_{\alpha\beta}^{\nu\pm} \frac{\partial x^\alpha}{\partial \xi^i} \frac{\partial x^\beta}{\partial \xi^j} \right), \quad (18)$$

where  $\eta_\nu$  are the units normal at the junction  $\Sigma$ . The symbol ' $\pm$ ' corresponding to the interior and exterior spacetime, and  $\xi^i$  represents the intrinsic co-ordinates on  $\Sigma$ . As a result we can write down the non-trivial components of the extrinsic curvature by using the metrics (1) and (16), are given by

$$K_\tau^{\tau+} = \frac{\frac{M}{R^2} + \ddot{R}}{\sqrt{1 - \frac{2M}{R} + \dot{R}^2}}, \quad (19)$$

$$K_\tau^{\tau-} = \frac{1}{\sqrt{\dot{R}^2 + (1 + aR^2)^{-2}}} \left[ \ddot{R} + \frac{aR [(2 + 6\omega) + (1 + \omega)(3aR^2 + a^2R^4)]}{2(1 + aR^2)^3} - \frac{(1 + \omega)\dot{R}^2 aR(6 + 3aR^2 + a^2R^4)}{2(1 + aR^2)(1 + 4aR^2 + 2a^2R^4)} \right], \quad (20)$$

$$K_\theta^{\theta+} = \frac{1}{R} \sqrt{1 - \frac{2M}{R} + \dot{R}^2}, \quad (21)$$

$$K_\theta^{\theta-} = \frac{1}{R} \sqrt{\dot{R}^2 + (1 + aR^2)^{-2}}, \quad (22)$$

where the overdot denotes derivative with respect to proper time  $\tau$ . Thus, the Lanczos equations [14] allow us to write the surface stresses, as follows:

$$\sigma = -\frac{1}{4\pi R} \left[ \sqrt{1 - \frac{2M}{R} + \dot{R}^2} - \sqrt{\frac{1}{(1 + aR^2)^2} + \dot{R}^2} \right], \quad (23)$$

and

$$\mathcal{P} = \frac{1}{8\pi R} \left[ \frac{1 - \frac{M}{R} + \dot{R}^2 + R\ddot{R}}{\sqrt{1 - \frac{2M}{R} + \dot{R}^2}} - \frac{(1 + \omega)\dot{R}^2 aR^2(6 + 3aR^2 + a^2R^4)}{2(1 + aR^2)(1 + 4aR^2 + 2a^2R^4)} + \frac{2 + (4 + 6\omega)aR^2 + (1 + \omega)(3a^2R^4 + a^3R^6)}{2(1 + aR^2)^3} + \dot{R}^2 + R\ddot{R}\sqrt{(1 + aR^2)^{-2} + \dot{R}^2} \right]. \quad (24)$$

The corresponding interpretation of  $\sigma$  as the energy-density, while  $\mathcal{P}$  as the tangential surface pressure connected with the work done by the internal forces on the junction surface.

It is then necessary to use the conservation identity given by  $S_j^i|_i = [T_{\mu\nu}e_{(j)}^\mu n^\nu]^+_-$ , where  $n^\mu$  is the unit normal 4-vector to  $\Sigma$  and  $e_{(i)}^\mu$  are components of the holonomic basis vectors tangent to  $\Sigma$ , where we are defining  $[X]^+_-$  the discontinuity across the junction surface i.e.,  $[X]^+_- = X^+|_\Sigma - X^-|_\Sigma$ .

From the above expression of conservation we can write  $S_\tau^i|_i = -[\dot{\sigma} + 2\dot{R}(\sigma + \mathcal{P})/R]$ , where the momentum flux term in the right hand side of the conservation identity is given by

$$[T_{\mu\nu}e_{(j)}^\mu n^\nu]^+_- = -\frac{(\rho + p_r)\dot{R}\sqrt{1 - 2m/R + \dot{R}^2}}{1 - 2m/R}. \quad (25)$$

where  $\rho$  and  $p_r$  may be deduced from Eqs. (3-4), respectively, evaluated at the junction radius,  $R$ . Further it is

easy to see from two Eqs. (23) and (24) that the energy conservation equation is fulfilled and can be recast as [29]:

$$\sigma' = -\frac{2}{R}(\sigma + \mathcal{P}) + \Xi, \quad (26)$$

where we are defining the prime operation as the derivative with respect to  $R$  and  $\Xi$  is given by

$$\Xi = -\frac{1}{4\pi R} \frac{(1+\omega)aR(6+3aR^2+a^2R^4)}{2(1+ar^2)(1+4aR^2+2a^2R^4)} \sqrt{(1+aR^2)^{-2} + \dot{R}^2}. \quad (27)$$

It is instructive to analyze the flux term [Eq. (27)] is zero when  $w = -1$ , which reduces to the analysis, see Ref. [19]. We now proceed with the surface mass of the thin shell is given by

$$m_s = 4\pi R^2 \sigma. \quad (28)$$

When one substitutes Eq. (23) into Eq. (28), one can get

$$m_s = -R \left[ \sqrt{1 - \frac{2M}{R} + \dot{R}^2} - \sqrt{\dot{R}^2 + (1+aR^2)^{-2}} \right], \quad (29)$$

Further, rearranging the above expression and evaluation at  $R = R_0$ , lead to the result of dark energy star, is given by

$$M = \frac{aR_0^3}{2} \frac{2+aR_0^2}{(1+aR_0^2)^2} + m_s(R_0) \left( \frac{1}{(1+aR_0^2)^2} - \frac{m_s(R_0)}{2R_0} \right). \quad (30)$$

Now, differentiating twice the expression in (28), and taking into account the radial derivative of  $\sigma'$ , we start by rewriting Eq. (26) in a convincing form

$$\left( \frac{m_s}{2R} \right)'' = \Upsilon - 4\pi \sigma' \eta, \quad (31)$$

where the unknown parameters are given by

$$\eta = \frac{\mathcal{P}'}{\sigma'}, \quad \Upsilon = \frac{4\pi}{R}(\sigma + \mathcal{P}) + 2\pi R \Xi'. \quad (32)$$

The expression found above will play an important role in stability analysis of static solutions. Here the parameter  $\eta$  is used to determine the stability of the system. There are ranges of the parameters  $\sqrt{\eta}$  for which the stability regions looks more convincing when  $0 < \eta \leq 1$ , so  $\eta$  can be interpreted as the velocity of sound on the shell.

In order to gain more impression we analyze our system by evolution identity and given by:  $\left[ T_{\mu\nu} n_{(j)}^\mu n^\nu \right]_-^+ = \bar{K}_j^i S_i^j$ , where  $\bar{K}_j^i = (K_j^{i+} + K_j^{i-})/2$ . The above discussion

leads to the evolution identity can be written as follows:

$$\begin{aligned} p_r + \frac{(\rho + p_r)\dot{R}^2}{1 - 2m/R} = \\ -\frac{1}{R} \left[ \sqrt{1 - \frac{2M}{R} + \dot{R}^2} + \sqrt{\frac{1}{(1+aR^2)^2} + \dot{R}^2} \right] \mathcal{P} \\ + \frac{1}{2} \left[ \frac{M/R^2 + \ddot{R}}{\sqrt{1 - \frac{2M}{R} + \dot{R}^2}} + \frac{1}{\sqrt{(1+aR^2)^{-2} + \dot{R}^2}} \times \right. \\ \left. \left( \frac{aR[2+6\omega+(1+\omega)(3aR^2+a^2R^4)]}{2(1+aR^2)^3} \right) \right. \\ \left. + \ddot{R} + \frac{aR\dot{R}^2(1+\omega)(6+3aR^2+a^2R^4)}{2(1+aR^2)(1+4aR^2+2a^2R^4)} \right] \sigma \end{aligned} \quad (33)$$

For the static solution at  $R = R_0$  with  $\dot{R} = \ddot{R} = 0$ , we can obtain the from of above equation the radial pressure in terms of the surface stress as :

$$\begin{aligned} p_r(R_0) = -\frac{1}{R_0} \left( \sqrt{1 - \frac{2M}{R_0}} + \frac{1}{\sqrt{1+aR_0^2}} \right) \mathcal{P} \\ + \frac{1}{2R_0^2} \left( \frac{M}{\sqrt{1 - \frac{2M}{R_0}}} + \frac{aR_0^3}{2(1+aR_0^2)^2} [(2+6\omega) \right. \\ \left. + (1+\omega)(3aR_0^2+a^2R_0^4)] \right) \sigma. \end{aligned} \quad (34)$$

We have seen that  $\sigma < 0$  and the shell pressure acting from the interior is negating  $p_r < 0$ , implying that the tension is in the radial direction. Therefore, a positive tangential surface pressure  $\mathcal{P}$  is required to keep the shell stable, i.e., hold it against collapsing.

#### IV. PHYSICAL PROPERTIES AND COMPARATIVE STUDY OF THE PHYSICAL PARAMETERS FOR COMPACT STAR MODEL

In order to obtain a stellar solution, the exact solutions of Einstein's field equations must satisfy some general physical requirements. Our goal is to explore the physical features of the strange dark star and determine the constraints for which the solutions are physically realistic. In next, we carry out a comparative study with the most recent observational data of number of compact stars given by Gangopadhyay et al. [37]. In the following we analyze in some detail the desirable physical properties of this star solution, in particular, free from physical and geometrical singularities, energy density and pressure are finite character at the origin  $r = 0$ , satisfying all the energy conditions at the stellar interior. We then proceed to solving them mathematically and discuss the obtained solutions with observational data, where we have considered the compact star Vela X - 1, estimated mass  $M = 1.77M_\odot$  and radius 9.56.

### A. Mass-radius relation and surface gravitational red shift

One can obtain the mass of the star within a radius  $r$  from Eq. (6). It is clear that the mass function  $m(r) \rightarrow 0$  as  $r \rightarrow 0$ , which indicated that mass function is regular at the center. The present paper highlights the maximum allowable mass-radius ratio for a static spherically symmetric perfect fluid sphere falls within the limit of  $< 8/9$  in [35] (in the unit  $c = G = 1$ ). Furthermore, considering the particular value of mass and radius for Vela X - 1, we obtain the variation of mass function in the stellar interior, which is depicted in Fig. 5. Note that the mass function represents a monotonic increasing function of ‘ $r$ ’ and  $m(r) > 0$  when  $0 < r < R$  i.e., within the radius of the star. Similarly assuming the estimated masses and radii for several compact objects such as X-ray pulsar Cen-X3, X-ray burster 4U 1538-52, and X-ray sources 4U 1538-52, we have performed a comparative study of the values of the physical parameters which is shown in Table I, and are closely equal to the observed values of most of the stars. Once again, we compared our solution of mass-radius relation for the different strange star, which do not cross the proposed range by Buchdahl in [35].

The compactness of the strange stars are found under the assumptions

$$u(r) = \frac{m(r)}{r} = \frac{ar^2}{2} \frac{2 + ar^2}{(1 + ar^2)^2}. \quad (35)$$

The compactness ( $u(r)$ ) of the star is a monotonic increasing function of  $r$  and the redshift function  $z_s$ , of the strange compact star can be defined through the equation

$$1 + z_s = (1 - 2u)^{-\frac{1}{2}}, \quad (36)$$

where the surface redshift function  $z_s$  is given by  $z_s = ar^2$ . We have calculated the maximum surface redshift ( $z_s$ ) for different strange stars from our model which shown in Table II. From the table it is clear that maximum value of the surface redshift,  $z_s < 1$ . So our result is compatible with the result obtained by [36].

### B. Energy Condition

In this section we are going to verify whether our particular model for dark energy star satisfies all the energy conditions or not, namely, null energy condition (NEC), weak energy condition (WEC), strong energy condition (SEC) and dominant energy condition (DEC), at all points in the interior of a star if the following inequalities hold simultaneously:

$$\text{NEC: } \rho(r) - p_r \geq 0, \quad (37)$$

$$\text{WEC: } \rho(r) - p_r(r) \geq 0, \quad \rho \geq 0, \quad (38)$$

$$\text{SEC: } \rho(r) - p_r(r) \geq 0, \quad \rho - p_r(r) - 2p_t(r) \geq 0, \quad (39)$$

$$\text{DEC: } \rho(r) > |p_r(r)|, \quad \rho > |p_t|. \quad (40)$$

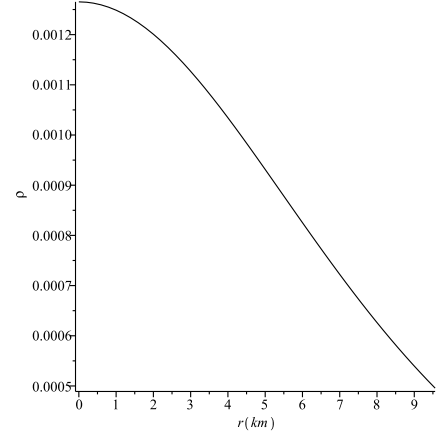


FIG. 1: Density variation in  $\text{GeV}/f\text{m}^3$  inside the star Vela X-1 with radial distance  $r$  in km.

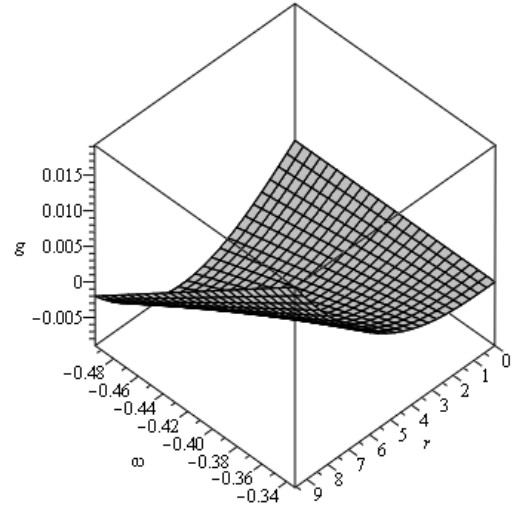


FIG. 2: The “gravity profile”,  $g(r)$ , is plotted against  $r$  when  $-1/3 < \omega < 0$ . Note that within the range of  $-1/3 < \omega < 0$ ,  $g(r) > 0$ , shows an inward gravitational attraction, so it is necessarily excluded for our dark star model.

We show the above inequalities with the help of graphical representation. In Fig. 6, we have plotted the L.H.S of the above inequalities which shows that our model satisfies these conditions for specific values of mass and radius at the stellar interior when  $\omega = -0.5$ .

### C. Stability Analysis

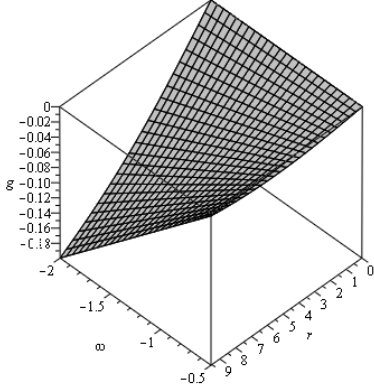
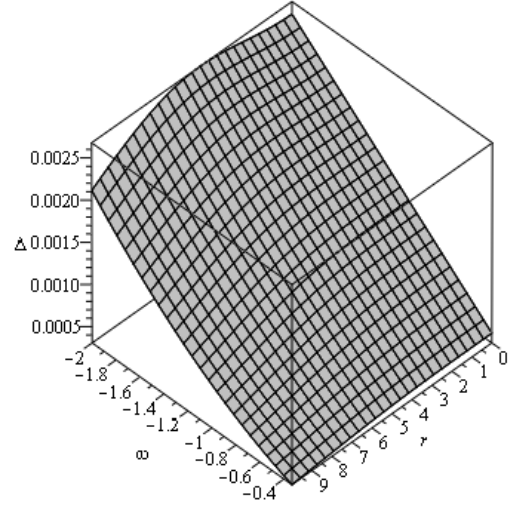
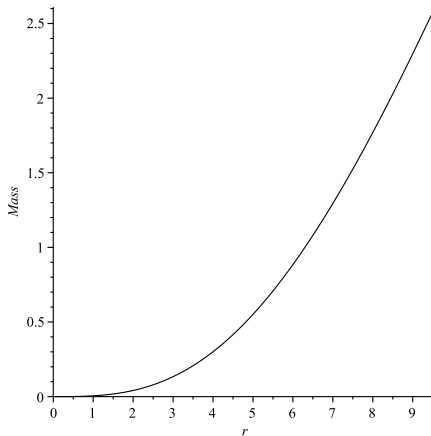
Let us now address the issue for stability analysis of the solution. In order to study the dynamical stability of the transition layer of these dark energy stars we consider a linear perturbation around those static solutions. It is interesting to note that if we want an equation of motion

TABLE I: Values of the constants  $a$ ,  $b$ ,  $H$  and  $K$  for different compact star models.

Compact Star	$a$	$R$ (km) observed	$M/M_\odot$ observed	$R$ (km) calculated	$M/M_\odot$ calculated	References
4U 1538-52	0.0037	$7.866 \pm 0.21$	$0.87 \pm 0.07$	7.87	0.90	Gangopadhyay <i>et al.</i> [37]
PSR J1614-2230	0.0062	$9.69 \pm 0.2$	$1.97 \pm 0.04$	9.7	1.97	Gangopadhyay <i>et al.</i> [37]
Vela X-1	0.0053	$9.56 \pm 0.08$	$1.77 \pm 0.08$	9.56	1.77	Gangopadhyay <i>et al.</i> [37]
Cen-X3	0.0046	$9.178 \pm 0.13$	$1.49 \pm 0.08$	9.18	1.5	Gangopadhyay <i>et al.</i> [37]

TABLE II: Values of physical parameters for different compact star models.

Compact Star	central density $\text{gm cm}^{-3}$	surface density $\text{gm cm}^{-3}$	$u$	$z_s$
4U 1538-52	$1.89 \times 10^{15}$	$0.72 \times 10^{15}$	0.168	0.228
PSR J1614-2230	$1.99 \times 10^{15}$	$0.68 \times 10^{15}$	0.299	0.579
Vela X-1	$1.71 \times 10^{15}$	$0.67 \times 10^{15}$	0.273	0.484
Cen-X3	$1.49 \times 10^{15}$	$0.67 \times 10^{15}$	0.241	0.389

FIG. 3: The “gravity profile”,  $g(r)$ , is plotted against  $r$  when  $-1/3 < \omega < 0$ , for our estimated mass and radius.FIG. 5: Anisotropy factor  $\Delta$  at the interior of the star for  $\omega < -1$ . We verify that  $\Delta > 0$  in the phantom region when  $\omega < -1$ , of strange stars Vela X - 1FIG. 4: Mass-radius relationship of strange stars Vela X - 1, which is characterised by the estimated mass  $M = 1.77M_\odot$  and radius 9.56. The estimated masses of several compact objects, whose properties are given in Table I.

of the thin shell, we obtain from Eq. (23), which reads

$$\dot{R}^2 + V(R) = 0, \quad (41)$$

with  $V$  (a) given by

$$V(R) = 1 - \frac{m(R) + M}{R} - \left( \frac{m_s(R)}{2R} \right)^2 - \left( \frac{M - m(R)}{m_s(R)} \right)^2. \quad (42)$$

Note that the potential function  $V(a)$  helps us to determine the stability region for the thin shell under our linear perturbation. Now we shall consider the Taylor series expansion around the static solution  $R_0$ , upto second

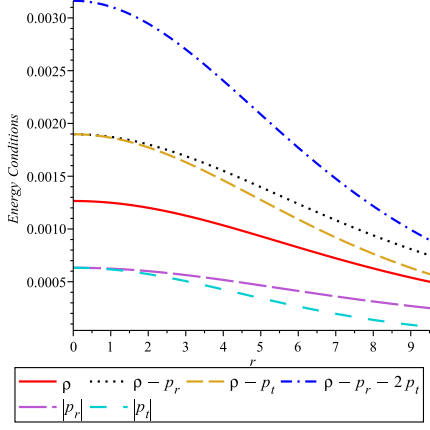


FIG. 6: Energy Conditions inside the strange star ‘Vela X-1’ is shown against  $r$ . From the figure it is clear that all the above mentioned energy conditions are satisfied by our model.

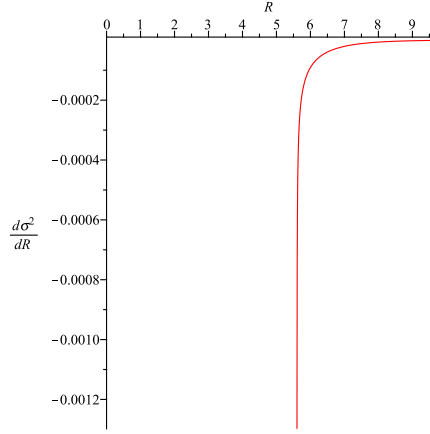


FIG. 7: ‘Vela X-1’ (radius  $R=9.56$ ): In these figure we have plotted the dimensionless parameter  $L = \frac{d^2 \sigma^2}{dR^2}$ . Therefore the stability region is constrained by the inequality (52).

order, we obtain

$$V(R) = V(R_0) + (R - R_0)V'(R_0) + \frac{(R - R_0)^2}{2}V''(R_0) + \mathcal{O}[(R - R_0)^3], \quad (43)$$

where prime corresponding to a derivative with respect to  $R$ . According to the standard method we are linearizing around the static radius  $R = R_0$ , we must have  $V(R_0) = 0$  and  $V'(R_0) = 0$ . It is straightforward to see that  $V'(R_0) = 0$  gives the relation

$$\left(\frac{m_s(R_0)}{2R_0}\right)' = \Phi = \frac{R_0}{m_s(R_0)} \left[ -\left(\frac{m(R_0) + M}{R_0}\right)' - 2\left(\frac{M - m(R_0)}{m_s(R_0)}\right)\left(\frac{M - m(R_0)}{m_s(R_0)}\right)' \right]. \quad (44)$$

With this definition the second derivative  $V''(R_0)$  can be written as

$$V'' = -\left(\frac{m + M}{R_0}\right)'' - 2\left[\left(\frac{m_s}{2R_0}\right)'\right]^2 - 2\left(\frac{m_s}{2R_0}\right)\left(\frac{m_s}{2R_0}\right)'' - 2\left[\left(\frac{M - m}{m_s}\right)'\right]^2 - 2\left(\frac{M - m}{m_s}\right)\left(\frac{M - m}{m_s}\right)''. \quad (45)$$

Thus, a static configuration demands that the first two terms of the Taylor series expansion vanish, and the first non-zero term in the expansion for equation of motion of the thin shell may be written as (considering the Eq. (41))

$$\dot{R}^2 + \frac{1}{2}V''(R_0)(R - R_0)^2 + \mathcal{O}[(R - R_0)^3] = 0, \quad (46)$$

To ensure the stability of static configuration at  $R = R_0$ , the second derivative of the potential function must be positive, i. e.,  $V''(R_0) > 0$ . For the sake of simplicity we rearrange the Eq. (45), which turns out

$$\Rightarrow V'' = \Pi - 2\Phi^2 - \frac{m_s}{R_0}(\Upsilon - 4\pi\sigma'\eta)\Big|_{R_0}. \quad (47)$$

In this regard, we proceed with notational simplicity, which turns out to be

$$\left(\frac{m_s}{2R}\right)'' = \Upsilon - 4\pi\sigma'\eta, \quad (48)$$

with

$$\Pi = -\left(\frac{m + M}{R_0}\right)'' - 2\left[\left(\frac{M - m}{m_s}\right)'\right]^2 - 2\left(\frac{M - m}{m_s}\right)\left(\frac{M - m}{m_s}\right)''. \quad (49)$$

We focus our attention on small velocity perturbations, thus assuming  $\eta(R_0) = \eta_0$  and using Eq.(47) for  $V''(R_0) > 0$  we have

$$\eta_0 \frac{d\sigma^2}{dR}\Big|_{R_0} > \frac{\sigma}{2\pi} \left[ \Upsilon + \frac{R_0}{m_s}(2\Phi^2 - \Pi) \right] = \Gamma \text{ (say)}. \quad (50)$$

Let us begin by examining the stable equilibrium regions by rewriting the Eq. (50), in the suggestive form as follows :

$$\eta_0 > \Gamma \left( \frac{d\sigma^2}{dR}\Big|_{R_0} \right)^{-1}, \quad \text{if} \quad \frac{d\sigma^2}{dR}\Big|_{R_0} > 0, \quad (51)$$



$$\eta_0 < \Gamma \left( \frac{d\sigma^2}{dR} \Big|_{R_0} \right)^{-1}, \quad \text{if} \quad \frac{d\sigma^2}{dR} \Big|_{R_0} < 0, \quad (52)$$

Let us make a comment concerning the dark energy stars by choosing specific mass functions, and deduce the stability region by considering the inequalities given in Eqs. (51-52). As it was pointed out in Ref. [14, 15], we can find the stability regions by the qualitative plots. The result is illustrated in Fig. 7, which indicates that the stability region is given below the surface by Eq. (52).

## V. RESULTS AND DISCUSSION

Black holes are well-established and generally accepted in relativity because of its strong astronomical evidence for their existence, though fundamental importance associate with black hole horizons introduce a number of theoretical problems which have not yet to be satisfactorily resolved. Therefore, it has been argued by several authors that after the gravitational collapse of massive stars, different objects could be formed other than black holes. One proposal, which was initiated recently, to dissolve the singularity and horizon problem is the gravastar (gravitational vacuum star) model proposed by Mazur and Mottola [6], has an effective phase transition at/near where the event horizon is expected to form. It has recently shown that one would ideally generalized the gravastar picture by matching an interior solution corresponding a dark energy equation of state, to an exterior Schwarzschild metric at a junction interface. Such a spherically symmetric model should not possess a horizon and it should process a static equilibrium solutions, sometime referred as a dark energy star (see for instance Ref. [14] for review).

We have studied the model describing compact gravitating configurations governed by the dark energy equation of state. We have analyzed the stellar configuration by imposing a specific choices of mass function, which is uniform in the stellar interior. The solutions set thus obtained are correlated with a set of astrophysical objects in connection to direct comparison of some strange/compact star candidates like X-ray pulsar Cen-

X3, X-ray burster 4U 1538-52, and X-ray sources 4U 1538-52. In order to compare the dark star with observational data, we specially considered the X-ray pulsar Vela X - 1, whose estimated mass  $M = 1.77M_\odot$  and radius 9.56. On substituting these values into the relevant equations we obtain the expression for energy density, radial and transverse pressures, gravity profile and anisotropic parameter for the model, where the energy density is maximum at the center and gradually decreases away towards the boundary (see Fig. (1)). All this results have been shown in more instructive way by graphical representation shown in Figs. 1-7.

Furthermore, we emphasize the results in more details, with observational data by Gangopadhyay *et al.* [37] of some well known pulsars like 4U 1538-52, PSR J1614-2230, Vela X - 1 and Cen X - 3. For this purpose, we produce data sheet for the purpose of comparison between present model stars and the known compact objects in Table I and II. It is to be noted that we have set  $G = c = 1$ , while solving Einstein's equations as well as for plotting all the figures. As one can see, the results extracted in this theory is very much compatible with the results obtained through the observations and the obtained ratio of mass-radius for different strange stars lies in the proposed range by Buchdahl [35]. Next, we examined the surface redshift ( $Z_s$ ) of the different compact stars are of finite values and vanishes out side of the star (see Table - II), which lies in the proposed range by Barraco & Hamity [36], are physically acceptable with those of observations. We concluded that it is possible to obtain the existence of dark energy stars, however, it is important to understand the nature and general properties of compact objects by through fine tuning.

## Acknowledgments

FR and AB would like to thank the authorities of the Inter-University Centre for Astronomy and Astrophysics, Pune, India for providing the research facilities. FR is also thankful to DST-SERB for financial support.

- 
- [1] G. Chapline : arXiv: astro-ph/0503200.
  - [2] G. Chapline, E. Hohlfeld, R. B. Laughlin and D. Santiago : *Phil. Mag. B*, **81**, 235 (2001).
  - [3] H. E. Stanley, (Oxford. U. Press, New York, 1971); C. Domb (Taylor and Francis, Bristol, PA, 1996).
  - [4] J. R. Oppenheimer and H. Snyder : *Phys. Rev.*, **56**, 455 (1939).
  - [5] M. A. Abramowicz *et al.* : *Astron. Astrophys.*, **396**, L31, (2002) [arXiv:astro-ph/0207270].
  - [6] P. O. Mazur and E. Mottola : arXiv:gr-qc/0109035; P. O. Mazur and E. Mottola : arXiv:gr-qc/0405111; P. O. Mazur and E. Mottola : *Proc. Nat. Acad. Sci.*, **111**, 9545 (2004).
  - [7] Dubravko Horvat *et al.* : *Class. Quant. Grav.*, **26**, 025003 (2009); R. Chan and M. F. A. da Silva : *JCAP*, **1007** 029 (2010).
  - [8] C. Cattoen, T. Faber and M. Visser : arXiv:gr-/0505137.
  - [9] N. Bili, G. B. Tupper and R. D. Viollier : arXiv:astro-ph/0503427.
  - [10] A. Grant *et al.* : *Astrophys. J.*, **560**, 49-71 (2001); S. Perlmutter, M. S. Turner and M. White : *Phys. Rev. Lett.*, **83**, 670-673 (1999).
  - [11] C. L. Bennett *et al.* : *Astrophys. J. Suppl.*, **148**, 1 (2003); G. Hinshaw *et al.* : *Astrophys. J. Suppl.*, **148**, 135 (2003).

- [12] G. Chapline, in Foundations of Quantum Mechanics, ed. by T. D. Black et al. (World Sci., Singapore, 1992).
- [13] J. Barbieri and G. Chapline : *Phys Lett. B*, , **590**, 8 (2004).
- [14] S. N. F. Lobo : *Class. Quantum. Grav.* , **23**, 1525 (2006); S. N. F. Lobo: *Phys. Rev. D* , **75**, 024023 (2007).
- [15] P. Bhar and F. Rahaman : *Eur. Phys. J. C*, **75**, 41 (2015).
- [16] A. K. Yadav, F. Rahaman and S. Ray : *Int. J. Theor. Phys.*, **50**, 871 (2011).
- [17] Stoytcho S. Yazadjiev : *Phys. Rev. D*, **83**, 127501 (2011); Dubravko Horvat and Anja Marunovic : *Class. Quant. Grav.*, **30**, 145006 (2013); F. Rahaman et al, : *Gen. Rel. Grav.*, **44**, 107-124 (2012).
- [18] W. Israel : *Nuovo Cimento*, **44B**, 1 (1966); and corrections in ibid., **48B**, 463 (1966).
- [19] M. Visser and D. L. Wiltshire : *Class. Quant. Grav.*, **21**, 1135 (2004).
- [20] A. R. Ruderman : *Astron. Astrophys.*, **10**, 427-476 (1972).
- [21] L. Herrera and N. O. Santos: *Phys. Report.*, **286**, 53 (1997).
- [22] R. L. Bowers and E. P. T. Liang : *Astrophys. J.*, **188** 657 (2004).
- [23] R. Kippenhahn, A. Weigert: *Springer*, Berlin 664 (1990).
- [24] A. I. Sokolov : *JETP* , **52**, 575 (1980).
- [25] R. F. Sawyer : *Phys. Rev. Lett.*, **29**, 382 (1972) .
- [26] J. Ponce de León : *Gen. Rel. Gravit.*, **25**, 1123 (1993).
- [27] H. A. Buchdahl : *Phys. Rev* , **116**, 1027 (1959).
- [28] F. Rahaman et al. : *Gen. Relativ. Gravit.* , **44**, 107 (2012).
- [29] F. S. N. Lobo and P. Crawford : *Class. Quant. Grav.* , **22**, 4869 (2005).
- [30] K. Bronnikov and J. C. Fabris : *Phys. Rev. Lett.*, **96**, 251101 (2006).
- [31] K. N. Singh, P. Bhar and N. Pant: *Int. J. Mod. Phys. D*, **25**, 1650099 (2016).
- [32] R. Chan et al. : *Gen. Relativ. Gravit.*, **41**, 1835 (2009).
- [33] S. W. Hawking, G. F. R. Ellis, "The Large Scale Structure of Spacetime" (Cambridge University Press, Cambridge, 1973).
- [34] E. Poisson and M. Visser : *Phys. Rev. D* , **52**, 7318 (1995); M. Ishak and K. Lake : *Phys. Rev. D* , **65**, 044011 (2002); E. F. Eiroa and G. E. Romero : *Gen. Rel. Grav.* , **36**, 651 (2004).
- [35] H. A. Buchdahl : *Phys. Rev. D* , **116**, 1027 (1959).
- [36] D. E. Barraco and V. H. Hamity : *Phys. Rev. D* , **65**, 124028 (2002).
- [37] T. Gangopadhyay et al. : *Mon. Not. R. Astron. Soc.* , **431**, 3216 (2013).